Sensors and Actuators B 235 (2016) 273–279

Contents lists available at ScienceDirect

Sensors and Actuators B: Chemical

journal homepage: www.elsevier.com/locate/snb

# Thermomechanical behavior of a bimaterial microchannel cantilever subjected to periodic IR radiation

N. Miriyala [a,b,*], M.F. Khan [a,b], T. Thundat [a,b]

[a] Ingenuity Lab, Edmonton, Canada
[b] Dept. of Chemical and Materials Engineering, University of Alberta, Edmonton, Canada

ARTICLE INFO

*Article history:*
Received 20 February 2016
Received in revised form 27 April 2016
Accepted 8 May 2016
Available online 10 May 2016

*Keywords:*
Microchannel cantilever
Photothermal cantilever deflection spectroscopy (PCDS)
Infrared spectroscopy of liquid
Thermomechanical behavior
Chemical selectivity

ABSTRACT

Here we report the thermomechanical response of a bimaterial microchannel cantilever (BMC) subjected to periodic heating by IR radiation. A detailed theoretical and experimental study was performed considering the BMC as a thermal sensor. Experiments were conducted to find out the thermal sensitivity and power sensitivity of various BMC designs. The thermal sensitivity of the BMC was found by monitoring the response of the BMC to external heating while the power sensitivity was measured by observing its behavior to varying incident IR power. We report a minimum measurement of 60 μW of power, an energy resolution of ~240 nJ and a temperature resolution of 4 mK using the BMC. The optimum BMC design was chosen to demonstrate a spectroscopy application to detect a minimum of 1.15 ng of ethanol in ethanol-water binary mixture. The purpose of this paper is to add molecular selectivity to the ultra-sensitive, novel design of microchannel cantilevers using photothermal spectroscopy techniques for biosensing applications.



## 1. Introduction

Microfabricated resonant beams have been extensively investigated as excellent gravimetric sensors for the detection of small quantities of basic ingredients of explosive chemicals [1], explosive materials [2], pathogens and for label- free detection of biomolecules [3,4], reaching single proton level mass resolution [5]. Though these resonators are highly successful in the detection of analytes in gaseous environments, they have received less attention in the detection of analytes in the presence of liquid. When a resonator is operated in a liquid environment, the frequency resolution and mass sensitivity are greatly affected due to damping and viscous drag effects inherent to such a system [6]. Recently, attempts have been made to weigh particles in a solution by designing an innovative resonator platform in which the liquid has been confined inside the resonator, while leaving the exterior to the gaseous environment or vacuum [7,8]. These so-called microchannel cantilevers have attracted wide attention because of their ability to measure the mass of a single bacterial cell and a nanoparticle in the solution [9], with a mass resolution of several attograms ($10^{-21}$ kg) [10]. The effective use of these microchannel cantilevers in the detection of biomolecules heavily depends on developing chemo-selective interfaces inside the microchannel using surface functionalization protocols [11]. Even though many functionalization protocols were developed for biosensing applications to bind to one particular analyte, the functionalized surface does not always guarantee 100% specificity to the targeted analyte. This is mainly because of the weak intermolecular interactions involved; especially in the functionalization process that are based on hydrogen bonding. Moreover, the efficiency of surface functionalization depends on the immobilization protocol and prior surface quality, the efficiency becomes even worse in the case of the detection of analyte in a mixture thus leading to unacceptable levels of false positives. In reality, these functionalization protocols are not only cumbersome but also add complexity and, in most instances, pose a threat to damage the device [12]. Recently, photothermal spectroscopy techniques have been investigated to address selectivity issues to overcome the difficulties associated with the surface functionalization [13,14]. Spectroscopy techniques are based on the unique molecular vibrational transitions in the mid-IR, or "molecular fingerprint", region where many molecules display characteristic peaks free from overtones, making them highly selective. Photothermal cantilever deflection spectroscopy (PCDS) combines the high thermal sensitivity of a bimaterial microcantilever with highly selective mid-IR spectroscopy. PCDS techniques were demonstrated to provide the molecular signature

* Corresponding author at: Ingenuity Lab, Edmonton T6G1Y4, Canada.
*E-mail address:* miriyala@ualberta.ca (N. Miriyala).

http://dx.doi.org/10.1016/j.snb.2016.05.043
0925-4005/

**Table 1**
Design specifications of the BMC designs in chip-A and chip-B.

| Parameter | Length (μm) | Width (μm) | Thickness t2 (nm) | Metal thickness t1 (nm) | Channel height (μm) | Channel width (μm) | Channel volume (pL) | Spring constant (N/m) |
|---|---|---|---|---|---|---|---|---|
| Chip-A | 600 | 76 | 1000 | 500 | 3 | 32 | 115.2 | 0.020 |
| Chip-B | 500 | 44 | 1000 | 650 | 3 | 16 | 48 | 0.208 |

**Table 2**
Summary of figures of merit of the BMC. The bold-faced font indicates the desired parameters for an ideal thermal sensor.

| Figure of merit | Definition | Formula | Chip-A | Chip-B |
|---|---|---|---|---|
| **Responsivity R (nm/mW)** | Quasi-static tip displacement per incident radiative power | $\frac{1}{P_\lambda}\frac{dz}{dx}$ | **7.4** | 5.1 |
| **Incident flux sensitivity $S_{IF}$, (10^(-5) nm μm²/mW)** | Tip displacement per incident radiative power, per illuminated cantilever area | $\frac{R}{A_{cant}}$ | 16.22 | **23.18** |
| **Noise equivalent power NEP, (μW)** | The limit on incident power that can be measured by the cantilever | $\frac{\sigma(\Delta z)}{R}$ | 202 | **60** |
| **Noise equivalent flux NEF, (10^(-3) μW/μm²)** | The incident radiative flux that produces a signal to noise ratio of one | $\frac{NEP}{A_{cant}}$ | 4.42 | **2.72** |
| **Detectivity (μm/μW)** | | $\sqrt{A_{cant}/NEP}$ | **1.05** | 2.47 |

from trace quantities of analytes on the sensor surface [15,16]. In a similar way, the photothermal nanomechanical IR spectrum of 5 wt% of ampicillin in a solution has been demonstrated using microchannel cantilevers [17]. This kind of research paves the way for the future biomolecule sensing in the presence of a liquid without chemical functionalization. Photothermal techniques study the photo-induced change in the thermal state of a material; therefore, the resonator under study should be considered as a thermal sensor and should possess high thermal sensitivity in order to respond to small temperature variations. Temperature sensitivity was introduced by depositing a metal layer of optimized thickness to the backside of the microchannel cantilever, effectively rendering it as a bimaterial microchannel cantilever (BMC). Due to the bimorph effect, the BMCs (with pico liter volume capacity) are very sensitive to temperature. In order to further extend the applications of these microchannel cantilevers as thermal sensors, we need to understand the thermomechanical behavior of these cantilevers, when subjected to thermal pulses. So far, extensive investigation on the optimization and performance of micro- optomechanical thermal sensors, based on bimaterial microcantilevers has been reported [18–22], but there is a lack of relevant information on the thermomechanical characterization of microchannel cantilevers.

In this paper, we have measured the thermomechanical response of two different BMC designs through periodic heating by IR radiation and we have also measured the response of the BMC to external heating. A detailed experimental analysis is presented to determine the minimum detectable photon radiation and minimum temperature detectable by the BMC. We also present methods for optimizing the sensor performance and explore the limits of sensor resolution based on fundamental noise calculations as presented in Table 2 of figures of merit. In this context, the figures of merit are the generalized benchmark values of a thermomechanical sensor that reflect the performance of the sensor on a standard scale. Finally we have implemented our parameter optimization method for the optimum BMC to determine the lowest detectable concentration of ethanol in a water-ethanol binary mixture using the PCDS technique.

## 2. Experimental

### 2.1. Materials and methods

A U-shaped microfluidic channel was fabricated on the top of a plain microcantilever. Both structures were fabricated using a low-pressure chemical vapor deposited (LPCVD) silicon rich nitride (SRN) material. The fabrication was done by employing bulk micromachining techniques using polysilicon as a sacrificial material. Required metal deposition was carried out using a thermal evaporator (Cressington, Ted Pella, Inc). Two BMC designs were investigated to determine the optimum design parameters. The schematic of the top view and the SEM cross section view of the BMC are shown in Fig. 1(a) and (b) respectively. The design parameters and dimensions of the BMC are presented in Table 1. The critical differences between the two designsare the microchannel dimensions and the channel volume. Complete details on the fabrication of the device and the set up to load liquid sample can be found elsewhere [23]. A quantum cascade laser (QCL) operating in the mid-IR range (6–13 μm) (Daylight Solutions, MIRCat), at 100 kHz repetition rate with 5% duty cycle was chosen as the IR source. The IR laser pulses from the QCL were modulated to an optimized count using a function generator (DS345 Stanford Research Systems, USA) and radiated upon the BMC. The static deflection of the BMC was measured using an optical lever method by employing a photosensitive detector (PSD) (SPC-PSD from SiTeck S2-0171). In order to record the deflection of the BMC, the amplitude signals from the PSD were sent to a lock-in amplifier (SR 850 Stanford Research Systems, USA). Deflection amplitude of the BMC to external temperature variation was measured by a data acquisition system (NI DAQ 2120) together with a temperature controller (Global lab PX9). The noise spectrum and resonance frequencies of the BMC were measured using a spectrum analyzer (Stanford Research Systems, Sunnyvale, CA).

### 2.2. Theory

Static bending of the BMC, due to a stress generated from a temperature induced thermal expansion mismatch between the layers, is calculated based on simple beam theory. It is assumed that the changes in the elastic module of the materials involved are negligible for small temperature changes involved in the current experiments. Though the BMC has a hollow channel on the top of the microcantilever, which affects heat transfer to and from the cantilever, the basic bimorph behavior was not greatly affected. Hence, the BMC was approximated to have two layers: one is the metal layer (subscript 1) and other is SRN (subscript 2).

The deflection of the BMC for a rectangular cantilever of length $l$, width $w$, and thickness $t$ is governed by the following equation [18]:

$$\frac{d^2z}{dx^2} = 6(\alpha_1 - \alpha_2)\left(\frac{t_1 + t_2}{{t_2}^2 K}\right)[T(x) - T_0] \quad (1)$$

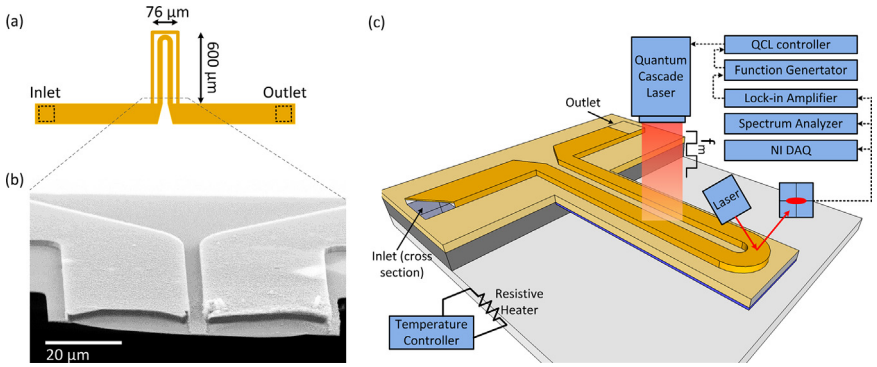


**Fig. 1.** (a) Schematic showing the top view of the BMC. Dimensions labeled are for the BMC on chip-A. (b) SEM micrograph of a cross-sectional view of the BMC at the anchor (viewed from the tip of the cantilever). Scale bar is 20 μm. (c) Schematic illustration of the experimental setup for measuring the power sensitivity using a modulated IR source and for measuring the thermomechanical sensitivity using Joule heating.

where

$$K = 4 + 6\left(\frac{t_1}{t_2}\right) + 4\left(\frac{t_1}{t_2}\right)^2 + \frac{E_1}{E_2}\left(\frac{t_1}{t_2}\right)^3 + \frac{E_2}{E_1}\left(\frac{t_2}{t_1}\right) \quad (2)$$

Here, $z(x)$ is the vertical deflection, $(T(x) - T_0)$ is the temperature gradient along the length of the BMC due to IR absorption, α is thermal expansion coefficient and $E$ is the Young's modulus. It is assumed that the temperature varies only along the length of the cantilever. Under steady state conditions where the IR power is uniformly absorbed over the entire length of the BMC, there exists a parabolic temperature profile along the length of the BMC [24]. The sensitivity of the BMC to IR radiation depends on the compliance of BMC, the rise in temperature due to IR absorption and the incident IR power. The sensitivity (S) of the BMC in steady state condition then becomes [18]:

$$S = \frac{z(0)}{P} = \frac{5}{4}(\alpha_1 - \alpha_2)\left(\frac{t_1 + t_2}{t_2{}^2 K}\right)\frac{L^3}{(\lambda_1 t_1 + \lambda_2 t_2)w} \quad (3)$$

where $P$ is the incident IR power, $z(0)$ is the deflection and λ is thermal conductivity.

From the above equation, the important parameters that affect the thermal sensitivity are mechanical compliance of the BMC, the length of the cantilever, the thickness of the metal layer, IR absorption characteristics of the BMC constituents and the power of the incident IR radiation.

### 2.3. Experimental setup for measuring the thermomechanical sensitivity

The thermomechanical sensitivity of the BMC with respect to external temperature was measured using a nanomechanical thermal analysis (NTA) set up as shown in Fig. 1(c). Deflection of the BMC was measured by monitoring the position of a laser beam (635 nm) reflected off of the BMC surface onto a PSD. It is to be noted that the laser is reflected from SRN surface as metal was deposited on the back of the cantilever. The BMC was mounted on a ceramic thermal chuck that was heated through a resistor element beneath the chuck. A *K*-type thermocouple was attached to the chuck near the BMC to measure the real-time temperature of the chuck. The chuck was heated from 30 °C to 50 °C at a heating rate of 2 °C/min and allowed to convectively cool from 50 °C to 30 °C at a cooling rate of 1.3 °C/min using a temperature PID controller for multiple cycles. The PSD signal was continuously monitored using a NI DAQ system. Electrical signals from the PSD were calibrated to real-time cantilever deflection (nm) by performing a calibration test using a plain bimaterial cantilever (without a microchannel) deflected under similar conditions of heating, using a topography measurement system (TMS) technique of the laser Doppler vibrometer (LDV) (Details of the calibration are presented in Supporting information Fig. S3). The thermal cycles of the entire chuck follow a temperature program that was in turn controlled by a temperature controller. The normalized deflection signals were recorded using a NI LabVIEW program that was capable of synchronizing with the temperature measurements from the temperature controller.

### 2.4. Experimental setup for measuring the power sensitivity

The BMC was placed in a cantilever holder and an experimental arrangement was made to radiate the BMC with a mid-IR QCL as shown in Fig. 1(c). The deflection amplitude signal from the PSD was diverted to a lock-in amplifier, locked at a frequency of 40 Hz. The QCL was also modulated at a modulation frequency ($f_m$) of 40 Hz using a function generator that was synchronized with the lock-in amplifier to radiate the BMC with periodic IR illumination. The peak-to-peak power output from the QCL, operating at a particular wavenumber, can be changed by providing different drive currents to the QCL. The relation between the drive current and the peak-to-peak power was provided with the QCL. Thus, the BMC was subjected to varying incident IR power and the deflections were monitored using a lock-in amplifier. The QCL was operated at a repetition rate of 100 kHz at a duty cycle of 5% which provided a maximum IR peak-to-peak power of 380 mW at 1270 $cm^{-1}$. It is to be noted that peak power from the QCL varies with IR wave number. A similar experimental setup was used for spectroscopy studies using a BMC holder that has a liquid loading arrangement.

### 2.5. Optimization of operational parameters

The thickness of the metal film is a critical parameter in determining the sensitivity of the BMC, as it dictates the deflection of the cantilever to the absorbed IR power. Lai et al. have shown that for a system of silicon nitride ($SiN_x$)/gold (Au), the maximum response was obtained for an optimum metal:$SiN_x$ thickness ratio of 1:4 [21]. They have also demonstrated a 50% improvement in the sensing response relative to previous publications by optimizing the thickness ratio of two materials [20,21]. Since our device has a microfluidic channel on top of the cantilever, the general optimum thickness ratio did not give maximum performance, possibly due to additional stiffness introduced by the aforementioned microchannel. The details of metal thickness optimization are presented in Supporting information (Fig. S2). Another important parameter that has profound effect on the sensitivity of the BMC is the IR modulation frequency. This frequency was optimized in such a way that IR radiation provides enough time for the BMC to respond to thermal pulses completely and also minimize noise in the

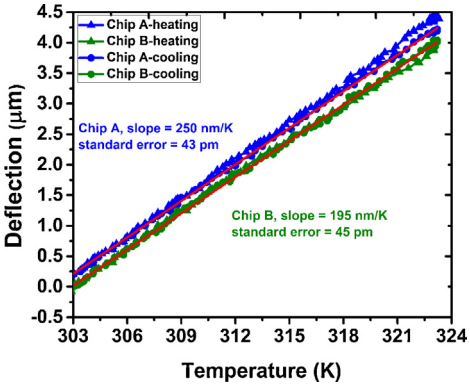


**Fig. 2.** Deflection of the BMC with respect to a change in external temperature while heating and cooling. Every chip has two curves, one with heating and the other with cooling cycle. It can be observed that the behavior of the BMC is reversed while heating and cooling, without much hysteresis. The red line indicates the linear fitting in all devices. The standard error is the error in fitting a straight line to the data. It can be seen that the BMC on chip-A and the BMC on chip-B have an almost similar thermal sensitivity of ~200 nm/K. (For interpretation of the references to colour in this figure legend, the reader is referred to the web version of this article.)

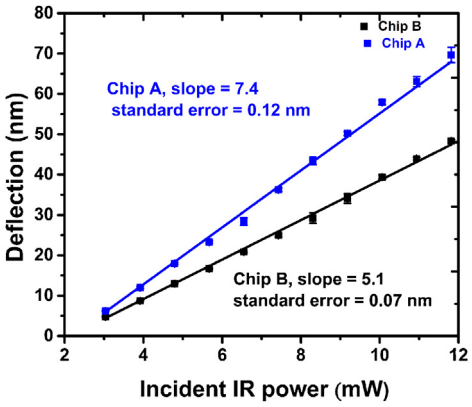


**Fig. 3.** Deflection of the BMC due to varying incident IR power. Each data point on the curve is an average of 15,000 data points recorded when the BMC is subjected to IR radiation at 1045 $cm^{-1}$, at a modulation frequency of $f_m$ = 40 Hz. The standard error is the error in fitting a straight line to the data. The noise in the measurement is depicted as error bars in the data points.

measurement. Therefore, the IR modulation frequency depends on the thermal time constant of the BMC. Details regarding the optimization of IR modulation are given in the Supporting information (Fig. S1).

## 3. Results and discussions

### 3.1. Measuring the thermomechanical sensitivity

The thermomechanical sensitivity of the BMC was measured by monitoring the deflection of the BMC as a function of external temperature as shown in Fig. 2. As the temperature of the chuck is increased, the BMC shows a linear increase in the PSD signal, indicating an upward bending of the cantilever followed by the reverse effect while cooling. The two curves of the same color in Fig. 2 correspond to the BMC deflection data obtained during heating and cooling thermal cycles. The heating program was optimized to provide enough time for thermal equilibrium at the end points of each cycle. The slope of the curve obtained for each BMC design gives the thermomechanical sensitivity of the BMC to external temperature. In this configuration, the BMC is assumed to be in a uniform temperature bath where the temperature gradient along the length of the BMC is constant. In this configuration, the BMC is essentially considered as a thermometer, thus one can estimate the temperature rise by looking at the deflection of the BMC [25]. These experiments were performed on both of the BMC designs to evaluate the effect of the design parameters listed in Table 1. From Fig. 2, it is evident that both of the BMC designs, on chip-A and chip-B, have identical thermal sensitivities of ~ 0.2 μm/K. The BMC on chip-A has a slightly better sensitivity when compared to the BMC on chip-B due to a longer length and lower compliance. The temperature resolution that can be measured using the BMC depends on its thermal characteristics and the noise in the measurement. The noise sources in our experimental set up are temperature fluctuations in the room, electrical noise and thermomechanical noise inherent to the BMC. The dominant source of noise, among all of the above mentioned is the thermomechanical noise of the BMC. We measured the amplitude of the thermomechanical noise of the BMC on chip-A to be ~ 2:5 pm using a lock-in amplifier which was locked at the resonance frequency of the BMC (Supporting information Fig. S4(b)). Considering a signal to noise ratio (SNR) of 3, the minimum temperature that can be measured using the BMC on chip-A is ~4 mK. Although better temperature resolution has been reported in literature, with values around ~$10^{-5}$ K, most of these reported values were theoretically predicted and associated with triangular shaped cantilevers [26] . The slightly poor thermal sensitivity of the BMC can be attributed to its design specifications, thick cantilever system, and higher noise associated with the BMC. Therefore, investigation of the BMC as a thermometer can provide an insight to explore exothermic or endothermic biochemical reactions in confined volumes.

### 3.2. Measuring the power sensitivity

The power sensitivity of the BMC was measured by monitoring the deflection of the BMC subjected to varying incident IR power as shown in Fig. 3. The IR radiation at 1045 $cm^{-1}$ wavenumber was modulated at a frequency of 40 Hz and the deflection of the BMC was recorded using a lock-in amplifier that is locked at the IR modulation frequency. Each data point on the line in Fig. 3 represents the average deflection signal of 15,000 data points. The solid line in Fig. 3 is the least square fit to the data. The slope of the line in Fig. 3 represents the power sensitivity (responsivity) of the BMC to incident IR power. As shown in Fig. 3, the responsivity of the BMC on chip-A to the incident IR power is 7.4 nm/mW, whereas the responsivity of the BMC on chip-B is only 5.1 nm/mW. From Fig. 3, it is evident that the BMC on chip-A has a higher power sensitivity than the BMC on chip-B. The higher sensitivity of the BMC on chip-A is attributed to the lower stiffness of the BMC and longer length as inferred from Eq. (3). However the BMC on chip-A has lower incident flux sensitivity ($S_{IF}$) than the BMC on chip-B as a result of its larger dimensions and larger channel volume, which affect the heat transport characteristics. Noise measurements were performed on both of the BMC designs to measure the noise in the BMC under the influence of IR as shown in the Supporting information. Note that the noise reported here is higher than the thermomechanical noise mentioned before. The increase in the noise when radiating the BMC with modulated IR might be due to the photothermal activation and thermal drift in the cantilever system. From the experimentally observed noise of 1.5 nm for the BMC on chip-A (Supporting information Fig. S5(a)), considering a SNR of 1 and the responsivity of 7.4 nm/mW, the minimum detectable IR power using the BMC on chip-A is found to be 202 μW. Since the time constant of the BMC on chip-A is ~4 ms, the estimated energy resolution is found to be ~800 nJ. Though the responsivity of the BMC on chip-A is greater, it acquired higher noise equivalent power (NEP) due to higher noise associated with long and slender cantilevers. The BMC on chip-B possesses better NEP and noise equivalent flux (NEF) due to extremely low noise (0.031 nm)

associated with stiffer cantilevers under the influence of IR. Hence, the BMC on chip-B can detect as low as 60 μW of incident IR power, even though it has lower sensitivity. The higher minimum IR power detectable by the BMC on chip-A is due to the larger noise associated with the longer BMC design despite the higher responsivity to incident IR. The average power of the IR source at 1045 $cm^{-1}$ and 1100 mA drive current incident on the BMC surface, neglecting the optical losses, is ~11.25 mW. The absorbed IR power ($Q_{abs}$) is calculated by the relation

$$Q_{abs} = Q_{inc}\alpha\frac{A_{cant}}{A_{spot}} \quad (4)$$

where $\alpha$ is the absorptivity of SRN at that thickness, $A_{cant}$ is the area of the cantilever, $A_{spot}$ is the area of the IR radiated spot with a diameter of 2 mm and $Q_{inc}$ is the incident IR power. The IR characteristics of the BMC are very much dependent on the cantilever dimensions, the thickness of constituent materials, and the absorptivity of the BMC at the radiated IR wavenumber. Though, there are not many published reports available on the IR spectral characteristics of cantilevers, the absorptivity of SRN in the mid-IR range in most publications was found to be 0.15 [27,28]. For the same input laser flux, the BMC on chip-A shows a larger response than the BMC on chip-B but the BMC on chip-B is more sensitive than the BMC on chip-A for a normalized absorbed power, calculated using Eq. (4). This is attributed to the smaller geometries of the BMC on chip-B to show better sensitivity to the absorbed IR power. All of the above mentioned figures are tabulated in Table 2 as the figures of merit for both of the BMC designs under periodic IR radiation. The definition and formula for each figure of merit are mentioned in Table 2 [24]. The desired figures of merit for a better IR thermal sensor in each category are represented in bold faced font.

For a typical analysis to know the temperature rise by the IR absorption in the case of the BMC on in chip-B, with an area of $500 \times 44\ \mu m^2$ and an absorption coefficient of 0.15, the absorbed power can be calculated as 11.81 μW. Assuming 80% of the photon energy is converted into heat due to non-radiative photon decay, the BMC produces a deflection of ~50 nm. As previously mentioned, the thermal sensitivity of the BMC under similar experimental conditions was 200 nm/K. From these calculations we find that the temperature rise due to absorbed IR radiation at 1045 $cm^{-1}$ is approximately 250 mK. From the above discussion, it can be understood that the miniscule mass of the BMC is susceptible to very small changes in temperature. Hence, micromechanical temperature sensors have to be made of materials that have low density, low specific heat, and cover large areas as identified in the case of uncooled IR detectors [29]. In summary, long cantilevers with low compliance and high IR absorption are more sensitive to incident IR, but they do not always have the best figures of merit. It is important to consider that long and slender geometry increases the noise and has adverse effects on power resolution and mass resolution. Ultimately, one should aim to achieve a balance between mass sensitivity and thermal sensitivity in order to obtain quantitative and qualitative information.

### 3.3. Photothermal IR spectroscopy using BMC

To investigate the effect of the design and the operational parameters optimization on the limit of spectroscopy, we performed spectroscopy of ethanol in water-ethanol binary mixtures using the BMC. Ethanol was taken as an example because of its simplicity in loading and preparing in different concentrations. Ethanol-water binary mixtures were prepared in different concentrations of ethanol in water, ranging from 20 wt% to 1 wt%. The BMC was loaded with a specific concentration of ethanol-water binary mixture and subjected to a pulsed IR wavenumber scan from 1204 $cm^{-1}$ to 960 $cm^{-1}$. Ethanol has two significant IR

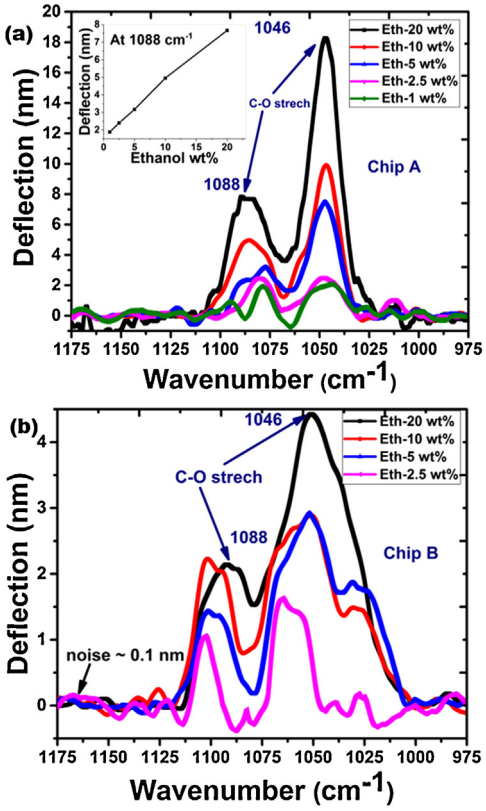


**Fig. 4.** Photothermal IR spectra of ethanol at various ethanol concentrations, in an ethanol-water binary mixture, obtained by monitoring the static deflection of the BMC to IR wavenumber scan, modulated at 15 Hz using a) the BMC on chip-A and b) the BMC on chip-B. Two signature IR peaks of ethanol due to C—O bond stretching can be observed. The inset in (a) shows the linear relationship of deflection amplitude with respect to ethanol concentration at 1088 $cm^{-1}$, indicating a typical spectroscopy behavior. The relative background noise of the BMC with ethanol with respect to water was found to be ~0.1 nm.

absorption peaks due to C—O stretch at 1046 $cm^{-1}$ and 1088 $cm^{-1}$ [30]. The scan rate was adjusted to 5 $cm^{-1}$/s to emphasize the fast measurement throughput of the current BMC system. The entire experiment, starting from sample loading to recording the scan data, takes place within ~2 min (50 s for scanning). A measurement baseline of a BMC loaded with water was taken for every new ethanol-water binary mixture introduced to the BMC. Fig. 4 depicts the deflection of the BMC with respect to IR wavenumber. From Fig. 4, it is evident that the deflection of the BMC is higher at the wavenumbers where the constituents in the channel absorb IR and eventually result in temperature rise. The molecules in the BMC constituents undergo molecular resonance with the incoming IR radiation, which causes the molecule to absorb IR at that particular wavenumber that is specific to the molecular bond configuration. Fig. 4(a) indicates the photothermal IR spectrum of ethanol-water binary mixture when loaded in the BMC on chip-A. From Fig. 4(a) a continuous decrease in the characteristic peaks of ethanol is observed with respect to the decrease in the concentration of ethanol. The inset in Fig. 4(a) shows a decrease in peak amplitude at 1088 $cm^{-1}$ with respect to a decrease in ethanol concentration, showing the linear behavior of spectroscopy. Fig. 4(b) shows the photothermal IR spectrum of an ethanol-water binary mixture when loaded in the BMC on chip-B. It is to be noted that photothermal IR spectrum of ethanol is presented only up to a concentration of 2.5 wt%. After this concentration, the characteristic IR peaks of ethanol are indistinguishable, indicating that this is the minimum concentration that can be detected using the BMC on chip-B. However, in the case of the BMC on chip-A,

characteristic IR peaks of ethanol are distinguishable up to a concentration of 1 wt% (~1.15 ng). The lower limit of detection in the case of the BMC on chip-A is attributed to higher sensitivity, higher channel volume, and lower stiffness relative to the BMC on chip-B. This indicates that the current BMC on chip-A can detect ~ 1.15 ng of ethanol in 113.85 ng of water background. In our earlier work [17], a wavenumber step scan was used to detect concentrations as low as 5 wt% ethanol in an ethanol-water binary mixture using a much higher powered IR laser, whereas here we report the detection of 1 wt% of ethanol at a lower IR power and a much faster measurement time. This is an order of magnitude improvement from the previous publication, with higher throughput.

## 4. Conclusions

Photothermal spectroscopy techniques can be used to impart chemical selectivity to microchannel cantilevers, targeted towards biosensing applications. We have provided a detailed analysis of the factors affecting the performance of a BMC when used as a thermal sensor. Several figures of merit were measured, such as responsivity, incident flux, noise equivalent power, noise equivalent flux, detectivity and thermal sensitivity. We have demonstrated the parameter optimization required to detect molecular signatures from as low as ~1.15 ng of the target analyte. The analysis provided in this report demonstrates a minimum measurement of 60 μW of power, an energy resolution of ~ 240 nJ, and a temperature resolution of 4 mK. Efforts are underway to improve the resolution by minimizing the noise in the measurement and improving the response of the BMC to periodic IR. The BMCs can hold small volumes (~pL) of liquid samples in confined geometry and possesses the ability to provide simultaneous information on density, viscosity, and molecular signature (using photothermal spectroscopy). We emphasize that such analysis would be useful for researchers using BMCs in applications such as biosensing, and is fundamental to understanding of biochemical reactions in confined volumes.

## Acknowledgements

This work is supported by the Canada Excellence Research Chair (CERC) program. The authors would like to thank Priyesh Dhandharia and Dr. Ankur Goswami for their help in quality discussions.

## Appendix A. Supplementary data

Supplementary data associated with this article can be found, in the online version, at http://dx.doi.org/10.1016/j.snb.2016.05.043.

## References

[1] L.A. Pinnaduwage, T. Thundat, J.E. Hawk, D.L. Hedden, P.F. Britt, E.J. Houser, S. Stepnowski, R.A. McGill, D. Bubb, Detection of 2,4-dinitrotoluene using microcantilever sensors, Sens. Actuators B: Chem. 99 (May (2–3)) (2004) 223–229.
[2] L.A. Pinnaduwage, V. Boiadjiev, J.E. Hawk, T. Thundat, Sensitive detection of plastic explosives with self-assembled monolayer-coated microcantilevers, Appl. Phys. Lett. 83 (August (7)) (2003) 1471–1473.
[3] N.V. Lavrik, M.J. Sepaniak, P.G. Datskos, Cantilever transducers as a platform for chemical and biological sensors, Rev. Sci. Instrum. 75 (July (7)) (2004) 2229–2253.
[4] A. Boisen, S. Dohn, S.S. Keller, S. Schmid, M. Tenje, Cantilever-like micromechanical sensors, Rep. Prog. Phys. 74 (March (3)) (2011) 036101.
[5] J. Chaste, A. Eichler, J. Moser, G. Ceballos, R. Rurali, A. Bachtold, A nanomechanical mass sensor with yoctogram resolution, Nat. Nanotechnol. 7 (May (5)) (2012) 301–304.
[6] J. Tamayo, A.D.L. Humphris, A.M. Malloy, M.J. Miles, Chemical sensors and biosensors in liquid environment based on microcantilevers with amplified quality factor, Ultramicroscopy 86 (January (1–2)) (2001) 167–173.
[7] T.P. Burg, S.R. Manalis, Suspended microchannel resonators for biomolecular detection, Appl. Phys. Lett. 83 (September (13)) (2003) 2698–2700.
[8] T.P. Burg, A.R. Mirza, N. Milovic, C.H. Tsau, G.A. Popescu, J.S. Foster, S.R. Manalis, Vacuum-packaged suspended microchannel resonant mass sensor for biomolecular detection, J. Microelectromech. Syst. 15 (December (6)) (2006) 1466–1476.
[9] T.P. Burg, M. Godin, S.M. Knudsen, W. Shen, G. Carlson, J.S. Foster, K. Babcock, S.R. Manalis, Weighing of biomolecules, single cells and single nanoparticles in fluid, Nature 446 (April (7139)) (2007) 1066–1069.
[10] J. Lee, W. Shen, K. Payer, T.P. Burg, S.R. Manalis, Toward attogram mass measurements in solution with suspended nanochannel resonators, Nano Lett. 10 (July (7)) (2010) 2537–2542.
[11] M.G. von Muhlen, N.D. Brault, S.M. Knudsen, S. Jiang, S.R. Manalis, Label-free biomarker sensing in undiluted serum with suspended microchannel resonators, Anal. Chem. 82 (March (5)) (2010) 1905–1910.
[12] S. Kim, D. Lee, X. Liu, C. Van Neste, S. Jeon, T. Thundat, Molecular recognition using receptor-free nanomechanical infrared spectroscopy based on a quantum cascade laser, Sci. Rep. 3 (January) (2016) 2013.
[13] T.S. Biswas, N. Miriyala, C. Doolin, X. Liu, T. Thundat, J.P. Davis, Femtogram-scale photothermal spectroscopy of explosive molecules on nanostrings, Anal. Chem. 86 (November (22)) (2014) 11368–11372.
[14] D. Lee, S. Kim, T. Thundat, Detection of biological analytes using nanomechanical infrared spectroscopy with a nanoporous microcantilever, Proc. of SPIE, Nano-Bio Sensing, Imaging, and Spectroscopy vol. 8879 (2013), p. 88790Q-88790Q-5.
[15] A. Wig, E.T. Arakawa, A. Passian, T.L. Ferrell, T. Thundat, Photothermal spectroscopy of *Bacillus anthracis* and *Bacillus cereus* with microcantilevers, Sens. Actuators B: Chem. 114 (March (1)) (2006) 206–211.
[16] A.R. Krause, C.V. Neste, L. Senesac, T. Thundat, E. Finot, Trace explosive detection using photothermal deflection spectroscopy, J. Appl. Phys. 103 (May (9)) (2008) 094906.
[17] M.F. Khan, S. Kim, D. Lee, S. Schmid, A. Boisen, T. Thundat, Nanomechanical identification of liquid reagents in a microfluidic channel, Lab. Chip 14 (March (7)) (2014) 1302–1307.
[18] J.R. Barnes, R.J. Stephenson, C.N. Woodburn, S.J. O'shea, M.E. Welland, T. Rayment, J.K. Gimzewski, C. Gerber, A femtojoule calorimeter using micromechanical sensors, Rev. Sci. Instrum. 65 (December (12)) (1994) 3793–3798.
[19] P.G. Datskos, N.V. Lavrik, S. Rajic, Performance of uncooled microcantilever thermal detectors, Rev. Sci. Instrum. 75 (March (4)) (2004) 1134–1148.
[20] J. Varesi, J. Lai, T. Perazzo, Z. Shi, A. Majumdar, Photothermal measurements at picowatt resolution using uncooled micro-optomechanical sensors, Appl. Phys. Lett. 71 (July (3)) (1997) 306–308.
[21] J. Lai, T. Perazzo, Z. Shi, A. Majumdar, Optimization and performance of high-resolution micro-optomechanical thermal sensors, Sens. Actuators Phys. 58 (February (2)) (1997) 113–119.
[22] B. Kwon, C. Wang, K. Park, R. Bhargava, W.P. King, Thermomechanical sensitivity of microcantilevers in the mid-infrared spectral region, Nanoscale Microscale Thermophys. Eng. 15 (1) (2011) 16–27.
[23] M.F. Khan, S. Schmid, Z.J. Davis, S. Dohn, A. Boisen, Fabrication of resonant micro cantilevers with integrated transparent fluidic channel, Microelectron. Eng. 88 (August (8)) (2011) 2300–2303.
[24] B. Kwon, M. Rosenberger, R. Bhargava, D.G. Cahill, W.P. King, Dynamic thermomechanical response of bimaterial microcantilevers to periodic heating by infrared radiation, Rev. Sci. Instrum. 83 (January (1)) (2012) 015003.
[25] S. Shen, A. Narayanaswamy, S. Goh, G. Chen, Thermal conductance of bimaterial microcantilevers, Appl. Phys. Lett. 92 (February (6)) (2008) 063509.
[26] J.K. Gimzewski, C. Gerber, E. Meyer, R.R. Schlittler, Observation of a chemical reaction using a micromechanical sensor, Chem. Phys. Lett. 217 (January (5–6)) (1994) 589–594.
[27] B. Kwon, C. Wang, K. Park, R. Bhargava, W.P. King, Thermomechanical sensitivity of microcantilevers in the mid-infrared spectral region, Nanoscale Microscale Thermophys. Eng. 15 (1) (2011) 16–27.
[28] M.R. Rosenberger, B. Kwon, D.G. Cahill, W.P. King, Impact of silicon nitride thickness on the infrared sensitivity of silicon nitride-aluminum microcantilevers, Sens. Actuators Phys. 185 (2012) 17–23.
[29] P.G. Datskos, N.V. Lavrik, S. Rajic, Performance of uncooled microcantilever thermal detectors, Rev. Sci. Instrum. 75 (April (4)) (2004) 1134–1148.
[30] I. Doroshenko, V. Pogorelov, V. Sablinskas, I. Doroshenko, V. Pogorelov, V. Sablinskas, Infrared absorption spectra of monohydric alcohols, infrared absorption spectra of monohydric alcohols, Dataset Pap. Sci. 2013 (October) (2013), e329406.

## Biographies

**Naresh Miriyala** is currently a Ph.D. candidate in the Department of Chemical and Materials Engineering at University of Alberta, Canada. He received his M. Tech degree from Department of Metallurgy and Materials Science, Indian Institute of Technology, Bombay, India. His current research focusses on microelectromechanical systems (MEMS) design, fabrication and applications, novel materials for sensing and device applications.

**Dr. Faheem Khan** is currently CERC Postdoctoral Fellow in the Department of Chemical and Materials Engineering at University of Alberta, Canada. He received his Ph.D. degree in MEMS sensor design and fabrication from the Technical University of Denmark. He has developed various different types of sensors including MEMS based IR spectrometer and a calorimeter for applications in microfluidics.

**Thomas Thundat** is a Canada Excellence Research Chair professor at the University of Alberta, Edmonton, Canada. He is also a Research Professor at the UT, Knoxville, a visiting professor at the University of Burgundy, France, a Distinguished Professor at the Indian Institute of Technology, Madras, and Centenary Professor at the Indian Institute of Science, Bangalore. Prior to becoming the CERC Chair in Oil Sands Molecular Engineering, Dr. Thundat was a University of Tennessee-Battelle/Oak Ridge National Laboratory (ORNL) Corporate Fellow and led the Nanoscale Science and Devices Group at ORNL. He received his Ph.D. in physics from State University of New York at Albany in 1987. He has authored over 380 publications in refereed journals, 48 book chapters, and 40 patents. Dr. Thundat is an elected Fellow of the American Physical Society (APS), the Electrochemical Society (ECS), the American Association for Advancement of Science (AAAS), the American Society of Mechanical Engineers (ASME), the SPIE, and the National Academy of Inventors (NAI). Dr. Thundat's research is currently focused on novel physical, chemical, and biological detection using micro and nanomechanical sensors.